*Proceedings of the*
*Annual Stability Conference*
*Structural Stability Research Council*
*Louisville, Kentucky, April 13-16, 2021*

# Stability of concrete-filled composite plate shear walls exposed to non-uniform fire loading

Ataollah T. Anvari[1], Preshit Wazalwar[2], Saahastaranshu R. Bhardwaj[3], Amit H. Varma[4]

## Abstract

Concrete-Filled Composite Plate Shear Walls (C-PSW/CF), also referred to as SpeedCore walls, are being used as innovative shear walls in commercial high-rise buildings. These walls offer advantages such as modularity and construction schedule contraction. The cross-section of C-PSWs/CF consists of concrete-infill sandwiched between the steel faceplates, where the faceplates are tied together by steel tie bars. To assess the applicability of C-PSWs/CF, the stability of these walls against fire loading needs to be analyzed. During a fire event, elevated temperatures will result in a deterioration in the mechanical properties of steel and concrete. Such degradation can lead to stability related failure of walls under axial loads significantly lower than the wall capacity at ambient temperatures. Previous studies have focused on investigating the performance of C-PSWs/CF exposed to uniform fire loading. However, these walls may be exposed to non-uniform fire loading such that just one face of the wall would be exposed to fire. Parametric studies were conducted for C-PSWs/CF exposed to non-uniform fire loading. Results revealed that an asymmetric thermal gradient develops through the wall thickness. Bending along the walls' height happened due to asymmetric thermal expansion as well as a shift in the cross-section's center of stiffness. This can lead to global instability failure of slender walls under non-uniform fire loading even at low axial loads and low surface temperatures. Results and observations from the parametric studies were used to investigate the stability of the walls and provide a recommendation for design of C-PSWs/CF exposed to non-uniform fire loading.

## 1. Introduction

C-PSWs/CF, also known as SpeedCore, are considered for high-rise residential and commercial construction due to the advantages of modularity, expedited construction schedule and elimination of rebar congestion. These composite walls are popular in construction as they combine the structural properties and advantages of steel and concrete materials. The cross-section of C-PSWs/CF (see Fig.1) includes plain concrete infill sandwiched by steel plates. The steel plates reduce the need to erection and demolition of separate formwork. Steel plates are connected to each other through steel tie bars. Tie bars ensure the structural integrity of the system (Seo et al.

[1] Graduate Research Assistant, Purdue University, ataghipo@purdue.edu
[2] Engineer, Saiful Bouquet Structural Engineers, pwazalwar@saifulbouquet.com
[3] Assistant Professor, The University of Alabama, saahas.bhardwaj@ua.edu
[4] Karl H. Kettelhut Professor and Director of Bowen Laboratory, Purdue University, ahvarma@purdue.edu

2016) and serve as out-of-plane shear reinforcement (Bhardwaj and Varma 2017). Ties bar (or shear studs) welded to steel plates provide composite action between steel plates and concrete infill.

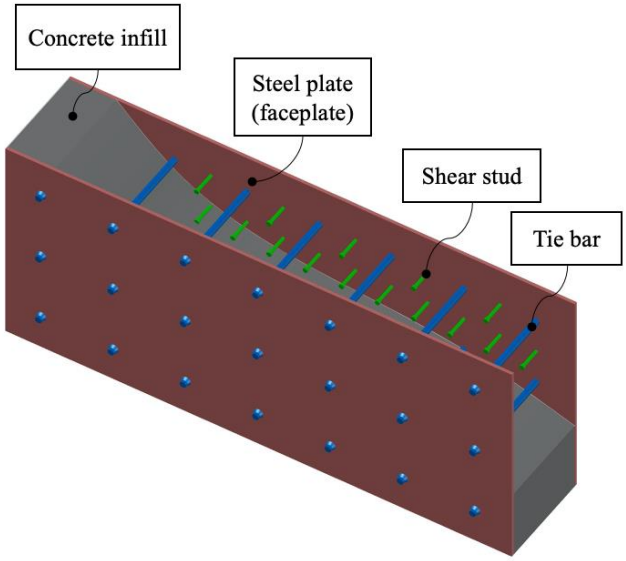


Figure 1: Details of the cross-section of a C-PSW/CF

Significant research has been done recently to study the behavior of C-PSWs/CF and provide design recommendations at ambient temperatures. The lateral capacity of C-PSWs/CF for wind and seismic loads has been investigated by Wang et al. (2018). The local buckling limit state of steel plates depends on steel plate slenderness, initial imperfections, and concrete casting pressure. Bhardwaj et al. (2018) recommended steel plate slenderness criteria for C-PSWs/CF. Bhardwaj and Varma (2016, 2017) developed a procedure to incorporate the effects of initial imperfections and concrete casting pressure on the compression behavior of C-PSWs/CF. The stability of empty steel C-PSWs/CF modules was evaluated by Varma et al. (2019). The current building codes, namely ASCE 7 (2016) and AISC 341 (AISC 2016) permit the use of C-PSW/CF in seismic regions (Bruneau et al. 2013, Alzeni and Bruneau 2014).

C-PSWs/CF can be directly exposed to elevated temperatures during a fire event. An important aspect of the applicability evaluation of the walls for commercial construction is the stability of these members under fire loading. During a fire incident, steel plates on the exterior of the composite walls will be directly exposed to fire temperatures in absence of fire protection. The mechanical properties of steel and concrete degrade significantly at elevated temperatures which can cause the reduction of stiffness and load-bearing capacity of structural members. Degraded material properties may cause crushing, local or global instability failure under gravity loads lower than the axial load-bearing capacity of a structural member at ambient conditions. Low thermal conductivity of concrete results in the generation of nonlinear thermal gradient over the cross-section of an axial composite member. Lower temperatures within the concrete infill can help to maintain the stability of the members. The concrete infill can resist a higher portion of the applied axial load under fire conditions and delay member failure (Anvari et al. 2020a).

Experimental and numerical studies have been conducted to investigate the behavior of C-PSWs/CF exposed to fire loading. Wei et al. (2017) experimentally tested Concrete-Filled Steel Plate Composite walls (CFSPC) exposed to uniform fire loading where CFSPC wall systems comprise the same elements as C-PSW/CF. Anvari et al. (2020b) tested axially loaded C-PSW/CF specimens exposed to elevated temperatures. The stability of C-PSWs/CF exposed to elevated temperatures has been studied numerically by Bhardwaj et al. (2019) and Anvari et al. (2020a). A design method was developed by Anvari et al. (2020b) to estimate the fire resistance rating and strength of the walls at elevated temperatures. The data from these research projects showed that wall thickness, wall height to thickness ratio, axial load ratio, and tie bar spacing have a major influence on the performance of C-PSWs/CF under uniform fire loading.

C-PSWs/CF in buildings typically have a width significantly more than the wall thickness. These walls can be exposed to uniform (both webs) heating, or non-uniform heating (one web) where the walls act as a fire barrier. Limited studies have been conducted on the performance of C-PSWs/CF exposed to non-uniform heating. Wei et al. (2017) tested four specimens for single-sided fire scenarios with one side of the wall exposed to fire. These specimens had a thickness of 150 and 200 mm and wall height to thickness ratios of 5 and 6.7, respectively. The fire resistance rating exceeded 2.5 hours where all specimens failed under the thermal insulation failure criterion (ISO 1999). Bhardwaj et al. (2019) developed finite element models simulating the performance of C-PSW/CF walls subjected to a combination of gravitational loads and non-uniform fire loading. Four 90 mm-thick specimens (wall height to thickness ratio = 13.3) with shear studs were tested by Wei et al. (2019). Three specimens globally buckled at elevated temperatures. Wei et al. (2019) recommended limiting the applied load and the load eccentricity to avoid early failure of walls.

The objective of the current study is to analytically investigate the stability of the C-PSWs/CF under non-uniform fire loading. A two-dimensional (2D) software tool was developed to model C-PSWs/CF under non-uniform fire loading. This software tool can aid in the performance-based design of C-PSWs/CF which would allow a more diverse range of structures to be designed. This tool permits a greater scope for optimization and innovation in the design of C-PSWs/CF. A parametric study was carried out to understand the effect of various parameters including wall height-to-thickness ratio, wall thickness, and axial load ratio on the stability of walls under non-uniform fire loading.

## 2. Two-dimensional analytical model

A two-dimensional fiber-based model was developed to investigate the behavior of C-PSWs/CF under non-uniform fire loading. The fiber-based analysis can provide a time-efficient and accurate tool for analyzing and designing composite axial members at elevated temperatures. General-purpose computing software (MathWorks, 2019) was used as the platform to develop the model.

The basic functionality of this tool was taken from the fiber model developed by Hong and Varma (2009) and Wazalwar et al. (2020). This model was found to be reasonably accurate in predicting the behavior and response of CFT columns and C-PSWs/CF under uniform fire loading. In the current study, the tool was upgraded to incorporate the analysis of C-PSWs/CF under non-uniform heating and was further validated based on the data obtained from the benchmarked finite element analyses by Anvari et al. (2020a). This tool is available for download from the Purdue University Research Repository (Varma et al. 2020).

In the current study, C-PSW/CF unit width columns modeling technique was used to build the fiber-based models of C-PSWs/CF. In this technique, the width of a wall can be discretized into unit width columns as shown in Fig. 2. Each C-PSW/CF unit width column has a thickness and width equal to the wall thickness and tie bar spacing, respectively. Thus, each unit is like a composite column with a steel plate on two faces and a concrete infill with tie bars distributed along the column's length. Anvari et al. (2020a) investigated the possibility of using C-PSW/CF unit width columns modeling technique to study the performance of walls under fire loading. They concluded that interior regions of a C-PSW/CF have a lower load-bearing capacity and stiffness than exterior regions. Thus, the unit width columns taken from the middle region of a wall can be used to conservatively estimate fire resistance of C-PSWs/CF at elevated temperatures. The calculated axial load capacity of the whole wall can be calculated by multiplying the capacity of a unit width column (from the interior region) by the total number of unit width columns along the wall width. The fire resistance rating of a unit width column can be considered as the whole wall's fire resistance rating.

Unit width columns of C-PSW/CF modeling technique was implemented in the developed software tool. Steel plates were modeled only on two sides of the concrete infill. Heat transfer was done only in one direction and temperature along the width and height was assumed to be constant. The heat was assumed to flow along the thickness of the unit width column. The fiber model was designed to simulate flexural buckling only about the horizontal axis, along with the wall width passing from the middle of the wall thickness.

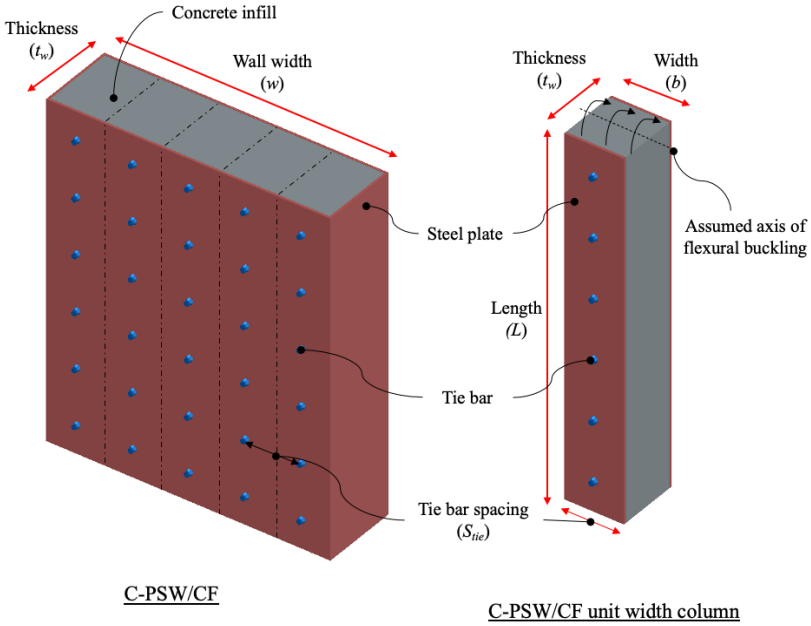


Figure 2: Geometric properties of a C-PSW/CF and unit width column

The 2D fiber model is a fundamental section-based model that represents the cross-section of composite axial members. The cross-section of a C-PSW/CF is divided into discrete fibers consisting of nodes and elements as shown in Fig. 3. The analysis is an incremental analysis wherein the member is analyzed in the present state at each time step. The analysis's results for every time step are used to update the member state for the subsequent time step. At every time

step, the procedure can be divided into three steps namely, (1) 2D heat transfer analysis, (2) section moment-curvature analysis and (3) non-linear column buckling analysis.

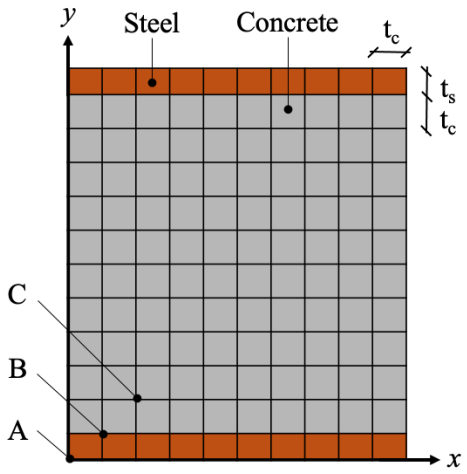


Figure 3: Discretized cross-section of a C-PSW/CF unit width column

The first step of the heat transfer analysis is to define the surface temperatures. The surface temperature can be calculated considering the convection and radiation onto the surface of the member. The heat transfer within the cross section is considered to be primarily through conduction. The surface temperatures along the height of the member are assumed to be constant. Thus, the calculated temperatures through a cross-section are valid for the entire height. The user can choose to specify the gas temperatures to calculate the surface temperature or specify the surface temperatures directly. The steps of the heat transfer analysis are presented in a flowchart shown in Fig. 4.

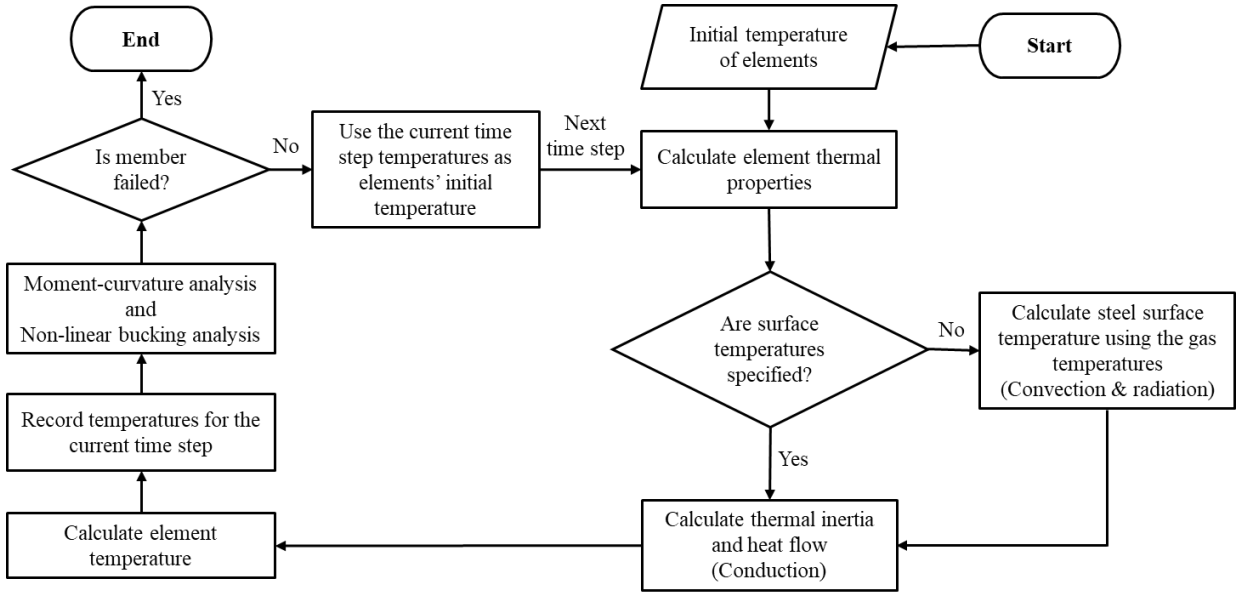


Figure 4: The procedure of calculating the temperature of nodes and elements across the cross-section of a member in 2D heat transfer analysis step

The heat balance equations between objects can be set up by considering all the contributions of heat transfer types namely, conduction, convection and radiation (Bergman et al. 2011). The heat balance equations in their finite difference form can be solved numerically (Lie and Irwin, 1995). The approximate finite difference heat balance equations developed by Hong (2007) are based on the theory presented by Lie and Irwin (1995). The heat balance equation follows a general form presented in Eq. 1. Examples of the utilized finite difference approximate heat transfer equations for three nodes are given in Table 1.

$$\text{Thermal inertia} = \text{Heat flow by conduction } (\dot{Q}_k) + \text{convection} (\dot{Q}_c) + \text{radiation} (\dot{Q}_r) \quad (1)$$

Table 1: Heat balance equations for nodes A, B and C

| Node | Thermal inertia | Conduction $(\dot{Q}_k)$ | Convection $(\dot{Q}_c)$ | Radiation $(\dot{Q}_r)$ |
|---|---|---|---|---|
| A | $\rho_s c_s^{T_{(i,j)}} \left(\frac{t_s t_c}{4}\right)(T^{n+1}_{(i,j)} - T^n_{(i,j)})\frac{1}{\Delta t}$ | $k_s^{T_{(i+1,j)}} \left(\frac{t_s}{2}\right)(T^n_{(i+1,j)} - T^n_{(i,j)})\frac{1}{t_c} +$ $k_s^{T_{(i,j+1)}} \left(\frac{t_c}{2}\right)(T^n_{(i,j+1)} - T^n_{(i,j)})\frac{1}{t_s}$ | $h(T^n_f - T^n_{(i,j)})\frac{t_c}{2}$ | $\sigma\varepsilon_s \left(\begin{matrix}\left(T^n_f + 273\right)^4 - \\ \left(T^n_{(i,j)} + 273\right)^4\end{matrix}\right)\frac{t_c}{2}$ |
| B | $\left(\rho_s c_s^{T^n_{(i,j)}} \left(\frac{t_c t_s}{2}\right) + \rho_c c_c^{T^n_{(i,j)}} \left(\frac{t_c^2}{2}\right)\right) \times (T^{n+1}_{(i,j)} - T^n_{(i,j)})\frac{1}{\Delta t}$ | $\left(k_s^{T_{(i+1,j)}} \frac{t_s}{2} + k_c^{T_{(i+1,j)}} \frac{t_c}{2}\right)(T^n_{(i+1,j)} - T^n_{(i,j)})\frac{1}{t_c} +$ $\left(k_s^{T_{(i-1,j)}} \frac{t_s}{2} + k_c^{T_{(i-1,j)}} \frac{t_c}{2}\right)(T^n_{(i-1,j)} - T^n_{(i,j)})\frac{1}{t_c} +$ $k_c^{T_{(i,j+1)}}(T^n_{(i,j+1)} - T^n_{(i,j)}) +$ $k_s^{T_{(i,j-1)}}(t_c)(T^n_{(i,j-1)} - T^n_{(i,j)})\frac{1}{t_s}$ | - | - |
| C | $\rho_c c_c^{T_{(i,j)}}(t_c^2)(T^{n+1}_{(i,j)} - T^n_{(i,j)})\frac{1}{\Delta t}$ | $k_c^{T_{(i+1,j)}}(T^n_{(i+1,j)} - T^n_{(i,j)}) +$ $k_c^{T_{(i-1,j)}}(T^n_{(i-1,j)} - T^n_{(i,j)}) +$ $k_c^{T_{(i,j+1)}}(T^n_{(i,j+1)} - T^n_{(i,j)}) +$ $k_c^{T_{(i,j-1)}}(T^n_{(i,j-1)} - T^n_{(i,j)})$ | - | - |

The second step of the analysis involves generating moment-curvature relation for the section using the current temperature state and the applied axial load. The section moment for each curvature value is calculated iteratively. The curvature is started from 0 $m^{-1}$ and increases in small increments. An initial centroidal strain ($\varepsilon_{cen}$) is assumed for a value of curvature ($\phi_i$) and the corresponding moment ($M_i$) for the cross-section is computed. The mechanical strains are obtained by subtracting thermal strains from total strains. Then the selected material stress-strain-temperature ($\sigma$-$\varepsilon$-$T$) relationship is used to calculate stresses in elements. Concrete strength in tension is assumed to be zero and strain hardening of steel in tension is also ignored. Net section moment is calculated by summing up the moment contribution of each element. The detailed steps of generating moment-curvature relation are as follows:

1- Calculate the total strain ($\varepsilon_{total}$) for every fiber (or element):

$$\varepsilon_{total(i,j)} = \varepsilon_{cen.} + \phi_i \times y_{(i,j)} \quad (2)$$

2- Calculate the thermal strain ($\varepsilon_{th}$):

$$\varepsilon_{th(i,j)} = \alpha_{(i,j)} \times \Delta T_{(i,j)} \tag{3}$$

3- Calculate the mechanical strain ($\varepsilon_{mech}$):

$$\varepsilon_{mech(i,j)} = \varepsilon_{total(i,j)} - \varepsilon_{th(i,j)} \tag{4}$$

4- Obtain the longitudinal stress ($\sigma_{(i,j)}$) from a selected stress-strain-temperature model based on the calculated mechanical strain

5- Calculate the axial force through the cross-section ($F_i$):

$$F_i = \sum \sigma_{(i,j)} \times A_{(i,j)} \tag{5}$$

6- Compare the calculated axial force ($F$) with the applied axial load ($P$):

- If the difference is within the defined tolerance, then the solution is converged.
- Otherwise, modify $\varepsilon_{cen}$ and go to Eq. 2

7- Calculate the moment ($M_i$) corresponding to the curvature ($\phi_i$):

$$M_i = \sum \sigma_{(i,j)} \times A_{(i,j)} \times y_{(i,j)} \tag{6}$$

8- Store $M_i$ and $F_i$ for $\phi_i$ and repeat the procedure for the incremented curvature ($\phi_{i+1}$).

The obtained moment-curvature relation is then used in column buckling analysis. The last step of analysis utilizes a modified version of Newmark's method of inelastic column buckling analysis to simulate the overall column behavior. Newmark's method is modified to be applicable for elevated temperatures by using the moment-curvature plots generated by section moment-curvature analysis. The member is discretized into several stations along the length. At each station, the section primary and secondary moments are obtained due to load eccentricity and lateral displacement, respectively. Load eccentricity is measured from the center of the stiffness of the cross-section, which may change with time due to member bending or non-uniform heating. To begin, a lateral deflected shape is assumed based on the column imperfection, and iterations are carried out at each time step to update the deflected shape. The calculated station moments are used to find the curvatures using moment-curvature relations. An updated deflected shape is then determined by twice numerically integrating these curvatures. This updated shape is compared to the assumed shape. Iterations are carried out until a converged deflected shape is obtained which satisfies all equilibrium equations. For non-uniform fire loadings, as material stiffness of steel and concrete reduces with increasing temperatures, center of stiffness of the section will vary with time. Hence center of stiffness of the section and load eccentricity are calculated at each time step, and the primary moment due to eccentricity is updated in modified Newmark's method.

The model checks for two modes of failure, namely global instability and yielding. The member fails due to global instability when the maximum moment along the column length exceeds the maximum moment that can be developed in the section or the maximum moment in the obtained $M$-$\phi$-$T$ relationships. The member is considered to fail in yielding if axial force equilibrium cannot be established at any step while generating the moment-curvature plot. Yielding failure mode governs for short (stocky) members whereas longer (slender) members typically undergo global instability failure. A diagram for various steps of the nonlinear buckling analysis is shown in Fig. 5.

The 2D fiber model is a quick and accurate tool for the analysis of C-PSW/CF. However, the model has certain limitations and simplifying assumptions. These major limitations and assumptions are discussed as follows:

- The fiber model provides only 2 degrees of freedom for strains, i.e. centroidal longitudinal strain and curvature, making it more restrictive than 3D models.
- The fiber model assumes plane sections remain plane and perpendicular to the neutral axis at every discrete location (station) along the length. Between two discrete points, section curvature is assumed to be interpolated.
- The fiber model uses uniaxial stress-strain-temperature models for steel and concrete. The multiaxial stresses and strains are not accounted for and are assumed to have no influence on the longitudinal (uniaxial) stress-strain-temperature behavior.
- As a result of the previous assumption, the fiber model does not consider the lateral pressure applied by concrete infill on steel plates (the consideration of which may increase their tendency to buckle outwards).
- Tie bars and shear studs are not modeled.

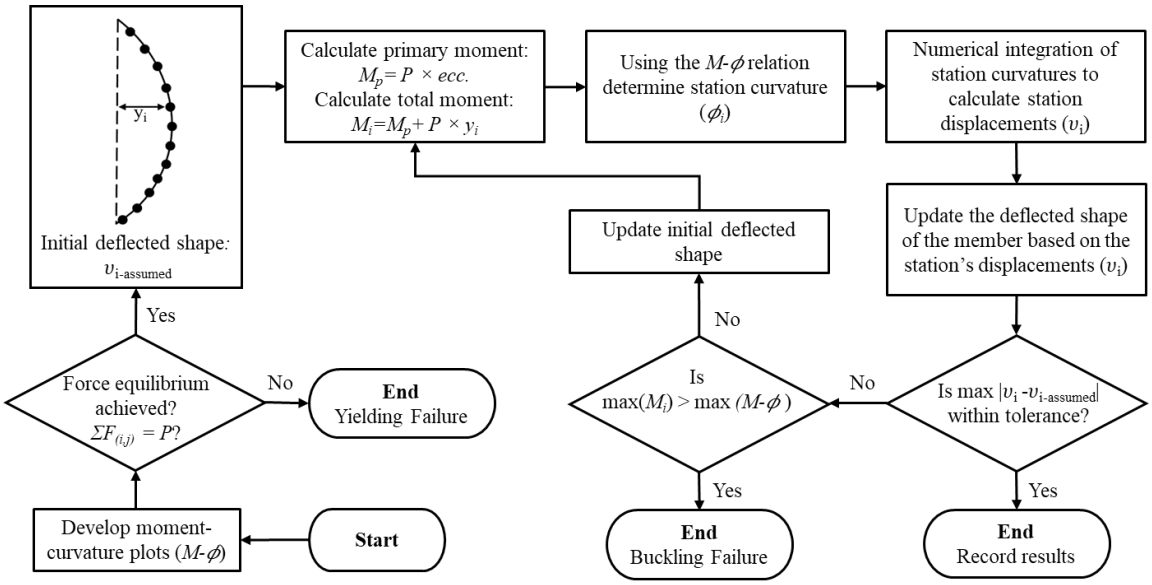

Figure 5: Flowchart for the procedure of nonlinear buckling analysis

## 3. 2D fiber-based model validation

The fiber model was extensively benchmarked by Hong and Varma (2009) and Wazalwar et al. (2020). The benchmarking process involved comparing the fiber model results with experimental and finite element analyses' data. Additional benchmarking analyses were conducted in the current study subjecting C-PSW/CF unit width columns to non-uniform fire loading. The temperatures and the displacements obtained from the fiber model were compared with those from with benchmarked FE models.

The temperature profiles across the section of C-PSW/CF unit width columns were compared with benchmarked 3D FE models. Fig. 6 shows the comparison of temperature profile through the thickness of a 300 mm thick C-PSW/CF unit width column at three time instants. The unit width column was exposed to uniform and non-uniform fire loading. As shown in Fig. 6(a), under

uniform fire exposure a non-linear symmetric temperature distribution occurred through the wall thickness with higher temperatures close to the surface. The obtained temperatures through the wall thickness for non-uniform fire exposure are compared in Fig. 6(b). The maximum temperature occurred at the exposed surface and the temperatures reduced nonlinearly with the coolest temperatures close to the unexposed surface. The minor discrepancies in the obtained temperatures are due to the application of different heat transfer methods and slight difference in material properties.

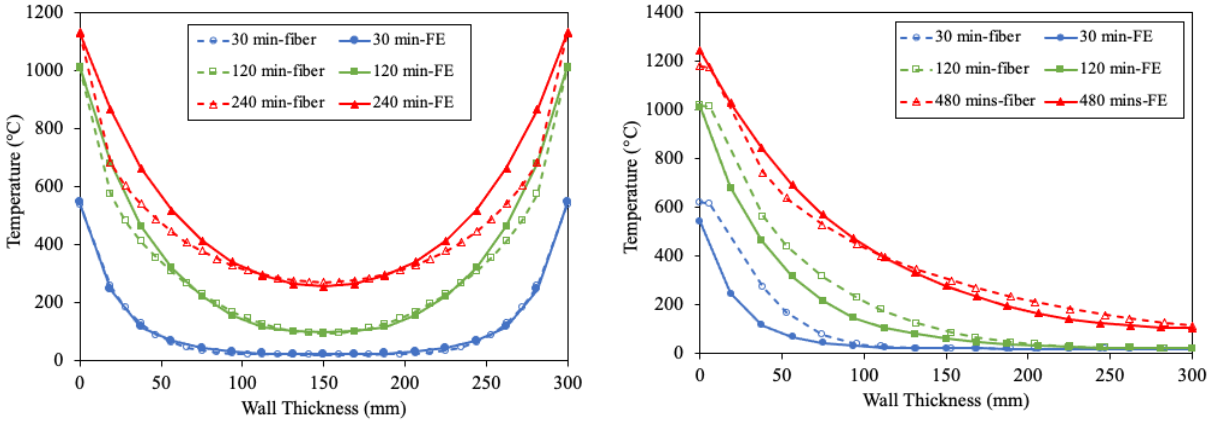


(a) (b)

Figure 6: Comparison of temperatures through wall thickness for (a) uniform and (b) non-uniform heating.

The axial displacements of C-PSW/CF unit width columns exposed to uniform (U) and non-uniform (NU) fire loading predicted by the fiber model were compared with data obtained from FE analysis. Figs. 7(a) and 7(b) present the axial displacements against time and surface temperature for four C-PSW/CF unit width columns, respectively. The unit width columns had a thickness of 200 and 300 mm and slenderness ratio (wall height-to-thickness ratio) of 10. An axial load equal to 20% of the zero-length compressive strength of cross-section ($A_g f'_c$) was applied. Table 2 presents a summary of the failure times and surface temperatures predicted by the developed fiber model and benchmarked FE models.

C-PSW/CF unit width columns experience large out-of-plane displacement under non-uniform fire loading. This out-of-plane displacement is due to the non-uniform expansion of material through the cross-section of walls. The development of large out-of-plane displacements due non-uniform fire loading of the walls is discussed in detail in the next section. To further validate the developed model the out-of-plane displacements obtained from the fiber-based model and FE models were compared as shown in Fig. 7(c) and (d). Figs. 7(c) and 7(d) shows the variation of out-of-plane displacement against time and the exposed surface temperature.

Table 2: Comparison of the failure time and surface temperature of C-PSW/CF unit width columns

| Nomenclature | $t_w$ | $L$ | $(L/t_w)$ | $t_p$ | Load | Time (min) | | Surface temperature (°C) | |
|---|---|---|---|---|---|---|---|---|---|
| | (mm) | (mm) | - | (mm) | $P/A_g f'_c$ | FE | fiber | FE | fiber |
| CW-200-10-20U | 200 | 2000 | 10 | 4 | 20% | 160 | 151 | 1068 | 1050 |
| CW-300-10-20U | 300 | 3000 | 10 | 6 | 20% | 277 | 284 | 1157 | 1155 |
| CW-200-10-20NU | 200 | 2000 | 10 | 4 | 20% | 310 | 260 | 1169 | 1144 |
| CW-300-10-20NU | 300 | 3000 | 10 | 6 | 20% | 751 | 636 | 1310 | 1288 |

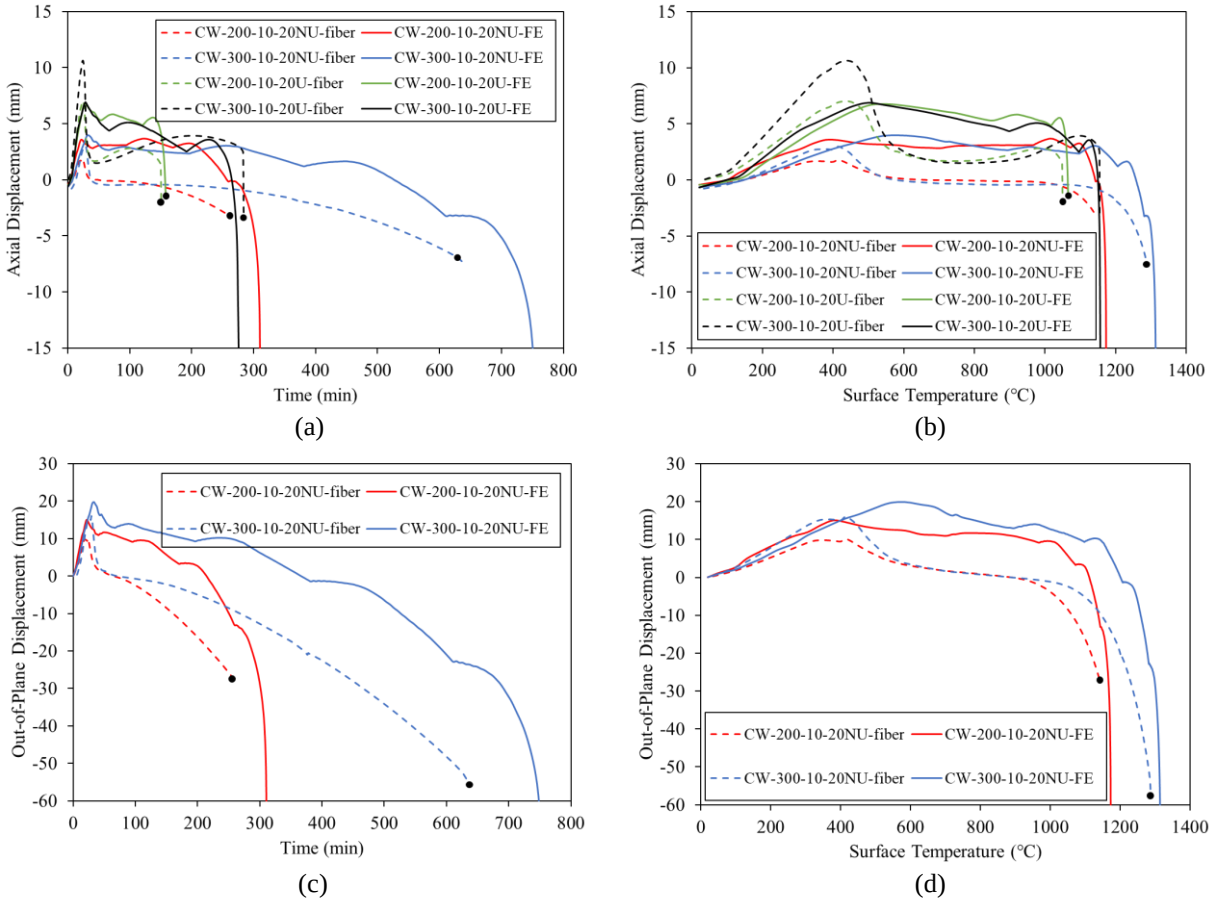


Figure 7: Comparison of axial displacements against (a) time and (b) surface temperature and out-of-plane displacements against (c) time and (d) surface temperature.

## 4. Parametric Study

The developed fiber model was used to carry out a parametric study on C-PSWs/CF exposed to non-uniform fire loading. The parameters considered were wall slenderness ratio ($L/t_w$ =10 - 25), wall thickness ($t_w$ = 200 - 400 mm) and applied axial load ratio (10% - 30% $A_g f'_c$). Table. 3 presents the details of C-PSW/CF unit width columns studied in the parametric study with failure time and temperature for each case. The faceplate thickness ($t_s$) ranged from 4 to 8 mm to maintain a cross section reinforcement ratio ($A_s/A_g$) equal to 4%. Steel plate's yield strength equal to 345 MPa and concrete infill's compressive strength equal to 40 MPa were considered in the model. Tie bar spacing ($S_{tie}$) was equal to half of wall thickness ($t_w/2$) for all cases. The gas temperature of the unit width columns followed ISO 834 (ISO, 1999) standard time-temperature curve.

C-PSW/CF unit width columns with a thickness of 200 to 400 mm were modeled. The thickness of C-PSWs/CF had a major influence on the performance of walls under fire loading. A comparison of failure time of unit width columns with various thicknesses indicated that the thinner walls failed earlier. In Fig. 8, the temperature profile of the walls is compared at 30 and 120 minutes. The temperatures through the wall thickness are plotted against the normalized distances (distance/wall thickness) to be able to compare the temperature profile of walls with various thicknesses in a single plot. Although the surface temperatures of the walls are similar, the temperature profiles through the thickness were varied. Thinner walls had a lower temperature

than the thicker walls. Due to the low thermal conductivity of concrete the temperature within the concrete infill raised at a lower rate.

Table 3: Parametric study matrix for C-PSW/CF unit width columns

| Nomenclature | Thickness ($t_w$) | Length ($L$) | Faceplate Thickness ($t_p$) | Slenderness ($L/t_w$) | Load ($\%A_g f_c$) | Fire scenario[+] | Time (min) | Surface temperature (°C) |
|---|---|---|---|---|---|---|---|---|
| CW-300-15-20U | 300 | 4500 | 6 | 15 | 20 | U | 175 | 1075 |
| CW-300-25-20U | 300 | 7500 | 6 | 25 | 20 | U | 75 | 918 |
| CW-300-10-20NU | 300 | 3000 | 6 | 10 | 20 | NU | 636 | 1288 |
| CW-300-15-20NU | 300 | 4500 | 6 | 15 | 20 | NU | 400 | 1214 |
| CW-300-20-20NU | 300 | 6000 | 6 | 20 | 20 | NU | 256 | 1141 |
| CW-300-25-20NU | 300 | 7500 | 6 | 25 | 20 | NU | 28 | 482 |
| CW-200-15-20NU | 200 | 3000 | 4 | 15 | 20 | NU | 199 | 1099 |
| CW-400-15-20NU | 400 | 6000 | 8 | 15 | 20 | NU | 677 | 1298 |
| CW-300-15-10NU | 300 | 4500 | 6 | 15 | 10 | NU | 1188 | 1385 |
| CW-300-25-10NU | 300 | 7500 | 6 | 25 | 10 | NU | 35 | 612 |
| CW-300-15-30NU | 300 | 4500 | 6 | 15 | 30 | NU | 164 | 1066 |

[*] All dimensions are in mm.
[+] U= uniform heating, NU= nonuniform heating

In Fig. 8, the temperature profile of a 300 mm-thick wall is compared under uniform and non-uniform fire exposure after 120 minutes of heating. For the case exposed to uniform fire loading, the average temperature of the elements through the wall thickness is higher than the walls exposed to non-uniform fire loading. The strength and the stiffness of concrete and steel material degrade at elevated temperatures. Thus, walls exposed to fire from uniform fire lose their stability earlier than the cases heated just on one face. A wall with a thickness of 300 mm, height to thickness ratio of 15 was analyzed under both uniform and non-uniform fire loading where it failed after 175 and 400 minutes respectively.

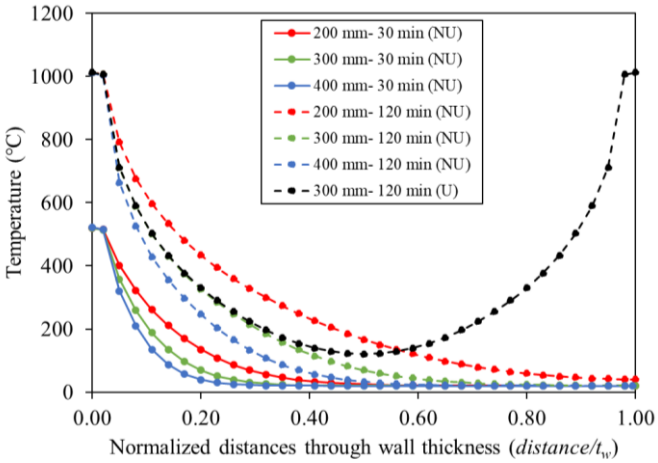

Figure 8: Temperature profile of the walls with a thickness of 200 to 400 mm at 30 and 120 minutes

Another observation from Table 3 is the difference in failure surface temperature and failure time for walls with various slenderness ratios ($L/t_w$). Walls with slenderness ratios greater than 20 ($L/t_w$ > 20) failed in a short time (or at low surface temperatures) while stocky walls were stable for a longer duration. Slender walls failed sooner because the generated moments due to asymmetric thermal gradients through the wall thickness led to instability even at lower temperatures. Due to asymmetric heating, the walls initially buckle in the direction of the heated face. This phenomenon is due to the heated steel faceplate expanding more than the remaining section. The out-of-plane displacements of 300 mm thick walls with slenderness ratios of 15 to 25 are compared in Fig. 9(a). The shorter walls ($L/t_w \leq 20$) were seen to buckle towards the unexposed face after a period of heating. The asymmetric heating results in more degradation in steel and concrete stiffness near the exposed face as compared to that near the unexposed face. Thus, the center of stiffness shifts towards the unexposed face. As the axial load is applied at the geometric center of the section, a moment ($M_{ecc}$) is generated which opposes the moment due to the expansion of the material on the exposed face ($M_{th}$). The wall section would buckle towards the unexposed face when the primary moment ($M_{ecc}$) overcomes the thermal moment ($M_{th}$) and the $P$-$\Delta$ effect due to thermal expansion. A representation of the two types of moments generated is shown in Fig. 9(b).

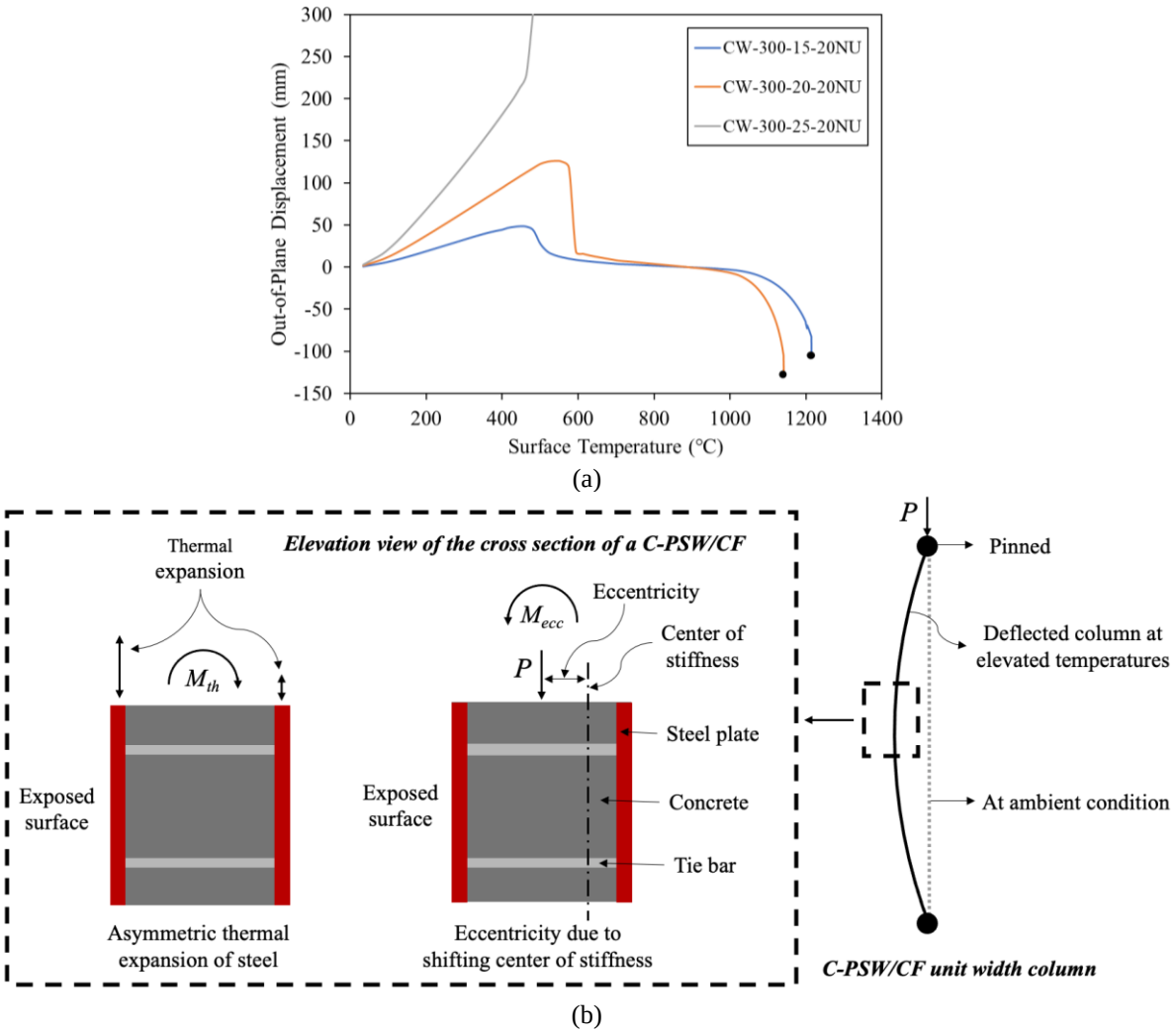


Figure 9. (a) Out-of-plane displacement of a 300mm thick wall with slenderness ratio of 15, 20 and 25. (b) Representation of the two types of moments generated in a wall section exposed to asymmetric heating.

C-PSWs/CF were also studied for axial load ratios ranging from 10 to 30% of $A_g f'_c$ to understand the relative effect of applied axial load. Axial load ratio had a major influence on the fire resistance of C-PSWs/CF wherein the fire resistance of the wall reduced significantly under higher axial load ratios. Fire resistance decreased rapidly as wall slenderness ratio ($L/t_w$) exceeded 20 irrespective of the applied axial load. The time to failure of the six models with 20% and 30% applied axial load is plotted in Fig. 10. The failure time for 20% and 30% $A_g f'_c$ nearly coincide for wall slenderness ratios ($L/t_w$) more than 20. For $L/t_w$ less than 20, the applied axial load had a significant effect on fire resistance rating. Wall sections with slenderness ratios less than 20, however, were seen to be stable for a longer duration.

Slender wall sections ($L/t_w$ > 20) failed quickly even for low applied axial loads. For a load ratio of 10% ($A_g f'_c$), the wall section ($t_w$ = 300 mm) failed after 35 minutes, at a surface temperature of 612 ℃ (see Table 3). Such a difference in behavior was not observed for symmetric fire loading (Anvari et al. 2020a) as thermal effects do not lead to thermal bowing when a member is heated uniformly. In such cases, moments may arise only because of imperfections in the member.

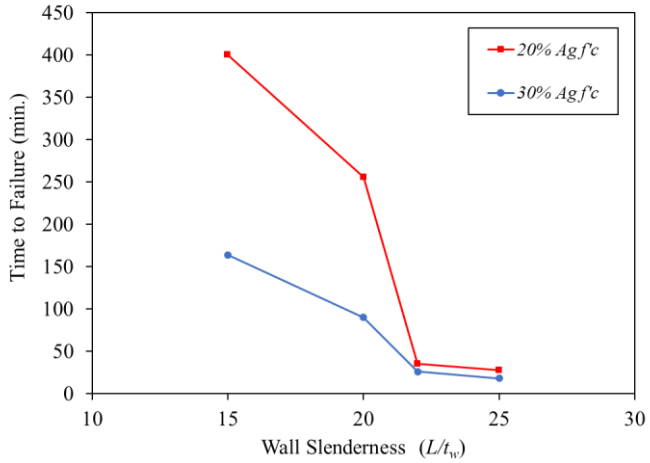


Figure 10: The variation of time to failure with wall slenderness ratios for 300 mm thick walls with an applied axial load equal to 20% and 30% $A_g f'_c$ subjected to non-uniform heating.

## 5. Conclusions

The performance of Composite-Plate Shear Walls/Concrete Filled (C-PSWs/CF) subjected to gravity and non-uniform fire loading was investigated in the current study. Understanding the behavior of C-PSW/CF systems under fire loading is essential to prevent or delay the failure of structures exposed to fire. During a fire event, the steel faceplate at the exterior surface of the wall would be directly exposed to fire and a non-linear thermal gradient will develop through the wall thickness. The mechanical properties of steel and concrete materials undergo degradation at elevated temperatures. Consequently, walls can lose their stability or load-bearing capacity under combined axial and fire loading. A cross-section behavior based 2D fiber-based analytical model was developed to simulate C-PSWs/CF under non-uniform fire loading. A single face of C-PSW/CF may be exposed to fire while the other side remains at ambient temperature. This model incorporated algorithms of heat transfer, calculation of moment-curvature response, and inelastic buckling. The fiber model was validated using benchmarked 3D FE results. The fiber model was used to conduct a parametric study to evaluate the effect of wall slenderness ratio (wall height-to-thickness ratio), wall thickness, and applied axial load ratio ($P/A_g f'_c$) on the stability of C-PSW/CF due to non-uniform heating.

The results from the parametric study indicate that wall slenderness ratio, wall thickness and applied load ratio have a significant influence on the fire resistance of walls. An increase in wall slenderness ratio had a detrimental effect on the performance of C-PSWs/CF at elevated temperatures. It was observed that walls with wall slenderness ratios greater than 20 have a low fire resistance under asymmetric heating, irrespective of the applied axial load. For instance, the fire resistance rating of walls ($t_w$ = 300 mm – 20% load) reduced from 256 min to 28 min as the slenderness ratio increased from 20 to 25. This premature failure of walls was due to second-order moments resulting from non-uniform thermal expansion caused by the asymmetric temperature gradient. Walls with slenderness less than 20 had a significantly higher fire resistance rating. Based on these observations, it is recommended to define a wall slenderness ratio limit of 20 for unprotected walls that would be exposed to asymmetric heating.

## Symbols

| | |
|---|---|
| $A_g$ | Gross section area of composite member |
| $A_{(i,j)}$ | Element area |
| $L$ | Length of the column |
| $M$ | Section moment |
| $S_{tie}$ | C-PSW/CF tie bar spacing |
| $T$ | Node temperature |
| $T_f$ | Temperature of fire |
| $c_c$ | Specific heat of concrete |
| $c_s$ | Specific heat of steel |
| $h$ | Heat convection coefficient |
| $k_c$ | Thermal conductivity of concrete |
| $k_s$ | Thermal conductivity of steel |
| $n$ | Time step number |
| $t_c$ | Concrete element thickness |
| $t_s$ | Steel element thickness |
| $t_w$ | Wall thickness |
| $y_{(i,j)}$ | Distance of an element to the neutral axis |
| $\Delta t$ | Duration of $n$th time step |
| $\alpha$ | Thermal expansion coefficient |
| $\rho_c$ | Mass density of concrete |
| $\rho_s$ | Mass density of steel |
| $\sigma$ | Stefan-Boltzmann constant |
| $\varepsilon$ | Strain |
| $\varepsilon_s$ | Emissivity of steel |


## Acknowledgments

The authors gratefully acknowledge the financial support provided by American Institute of Steel Construction (AISC), Charles Pankow Foundation and Steel Institute of New York (SINY).


## References


AISC (2016). *Seismic Provisions for Structural Steel Buildings.* AISC 341, American Institute of Steel Construction, Chicago, IL.

ASCE (2016). *Minimum Design Loads for Buildings and Other Structure.* ASCE 7, American Society of Civil Engineers, Reston, VA.

Alzeni, Y., Bruneau, M. (2014). "Cyclic Inelastic Behavior of Concrete Filled Sandwich Panel Walls Subjected to In-Plane Flexure," Technical Report MCEER-14-0009, MCEER, University at Buffalo, Buffalo, NY.

Anvari, A. T., Bhardwaj, S.R., Wazalwar, P, Varma, A. H. (2020a). "Stability of speedcore walls under fire loading: summary of numerical analyses." *Proceedings of the Annual Stability Conference-Structural Stability Research Council,* Atlanta, GA.

Anvari, A.T., Bhardwaj, S.R., Wazalwar, P., Varma, A.H. (2020b). "Structural Fire Engineering and Design of Filled Composite Plate Shear Walls or SpeedCore." Final Report, Charles Pankow Foundation, American Institute of Steel Construction and Steel Institute of New York. https://www.aisc.org/globalassets/aisc/research-library/final_report_cpsw_fire_design_cpf_03-18.pdf

Bergman, T. L., Incropera, F. P., DeWitt, D. P., Lavine, A. S. (2011). "Fundamentals of heat and mass transfer." John Wiley & Sons.

Bhardwaj, S.R., Sharma, S., Anvari, A. T., Varma, A. H. (2019). "On the stability of composite plate shear walls under fire loading." *Proceedings of the Annual Stability Conference - Structural Stability Research Council,* St. Louis, MO.

Bhardwaj, S.R., Varma, A.H. (2016). "Effect of Imperfections on the Compression Behavior of SC Walls." *Proceedings of the Annual Stability Conference - Structural Stability Research Council*, Orlando, FL.

Bhardwaj, S.R., Varma, A.H. (2017). "SC Wall Compression Behavior: Interaction of Design and Construction Parameters." *Proceedings of the Annual Stability Conference- Structural Stability Research Council,* San Antonio, TX.

Bhardwaj, S.R., Wang, A.Y., Varma, A.H. (2018). "Slenderness Requirements for CF-CPSW: The Effects of Concrete Casting." *Proceedings of Eighth International Conference on Thin-Walled Structures*, Lisbon, Portugal.

Bruneau, M., Alzeni, Y., and Fouché, P. (2013). "Seismic behavior of concrete-filled steel sandwich walls and concrete-filled steel tube columns." *Steel Innovations 2013 Conference*, Christchurch, New Zealand.

Hong, S. (2007). "Fundamental Behavior and Stability of CFT Columns Under Fire Loading", Doctoral dissertation, Purdue University.

Hong, S., Varma, A. H. (2009). "Predicting Fire Behavior of Composite CFT Columns Using Fundamental Section Behavior." *Journal of ASTM International*, 7 (1).

Lie, T.T., Irwin, R.J. (1995). "Fire Resistance of Rectangular Steel Columns Filled with Bar-Reinforced Concrete." *Journal of Structural Engineering*, 121 (5) 797–805.

ISO (1999). *Fire resistance tests-elements-elements of building construction*. ISO 834, International Standard ISO 834, Geneva, Switzerland.

MathWorks (2019). *MATLAB R2019b Documentation*, The MathWorks Inc., Natick, MA.

Seo, J., Varma, A. H., Sener, K., Ayhan, D. (2016). "Steel-plate composite (SC) walls: In-plane shear behavior, database, and design." *Journal of Constructional Steel Research*, 119 202-215.

Varma, A.H., Anvari, A.T., Wazalwar, P., Bhardwaj, S.R., Hariharan, H. (2020). "Fire design of SpeedCore walls and CFT columns." Purdue University Research Repository, https://purr.purdue.edu/publications/3473.

Varma, A. H., Shafaei, S., Klemencic, R. (2019). "Steel modules of composite plate shear walls: Behavior, stability, and design." *Thin-Walled Structures*, 145 106384.

Wang A., Seo J., Shafaei S., Varma A.H., and Klemencic, R. (2018). "On the Seismic Behavior of Concrete-Filled Composite Plate Shear Walls." *Eleventh U.S. National Conference on Earthquake Engineering*, Los Angeles, California.

Wazalwar, P., Bhardwaj, S.R., Anvari, A.T., Varma, A.H. (2020). "Stability of Composite Axial Members Under Fire Loading." *Proceedings of the Annual Stability Conference - Structural Stability Research Council*, Atlanta, GA.

Wei, F., Fang, C., Wu, B. (2017). "Fire resistance of concrete-filled steel plate composite (CFSPC) walls." *Fire Safety Journal*, 88 26-39.

Wei, F., Zheng, Z., Yu, J., Wang, Y. (2019). "Structure behavior of concrete filled double-steel-plate composite walls under fire." *Advances in Structural Engineering*, 22(8) 1895-1908.